Published in final edited form as:
Science. 2012 June 1; 336(6085): 1178–1181. doi:10.1126/science.1213368.

B Cell Signal Transduction in Germinal Center B Cells is Short-Circuited by Increased Phosphatase Activity

Ashraf M. Khalil[1], **John C. Cambier**[3], and **Mark J. Shlomchik**[1,2]

[1]Department of Laboratory Medicine, Yale University School of Medicine

[2]Department of Immunobiology, Yale University School of Medicine

[3]Integrated Department of Immunology, University of Colorado Health Sciences Center and National Jewish Health

Abstract

Germinal centers (GCs) generate memory B and plasma cells, essential for long-lived humoral immunity. GC B cells with high affinity B cell receptors (BCRs) are selectively expanded. To enable this selection, BCRs of such cells are thought to signal differently from those with lower affinity. We show that, surprisingly, most proliferating GC B cells did not demonstrate active BCR signaling. Rather, spontaneous and induced signaling was limited by increased phosphatase activity. Accordingly, both SHP-1 and SHIP-1 were hyperphosphorylated in GC cells and remained colocalized with BCRs after ligation. Furthermore, SHP-1 was required for GC maintenance. Intriguingly, GC B cells in the cell cycle G2 period regained responsiveness to BCR stimulation. These data have implications for how higher affinity B cells are selected in the GC.

T cell-dependent immune responses result in the selection of high affinity B cells, a process that occurs in the GC and depends on high-rate somatic mutation of V regions to generate variants. Resultant GC B cells can differentiate into either memory or plasma cells, which confer lasting humoral immunity (1). During this process, the BCR promotes the selective survival or expansion of higher affinity GC cells, but how this occurs is unclear. It is possible that BCRs on higher affinity GC B cells transduce a stronger, more sustained or qualitatively different signal. A second possibility is that higher affinity BCRs more effectively capture Ag, which is subsequently presented to helper T cells, resulting in higher affinity B cells obtaining more T cell-derived survival or proliferative signals (1, 2). Though BCR function is central to the process of GC B cell selection, BCR signaling in the GC is not well understood.

In vivo BCR signaling in GC B cells is of great interest, as these cells are activated and undergo continuous selection based on BCR affinity. Such study is complicated by the fact that GC B cells are rare, transient and heterogeneous. Furthermore, some GC B cells express an IgG-containing BCR, which mediates different signaling than the IgM BCR (3–5). Heterogeneity of affinity may also confer distinct signaling phenotypes on GC B cell BCR, which would be obscured in experiments utilizing assays of populations rather than single cells.

Corresponding author: Mark Shlomchik, Yale University School of Medicine, Department of Laboratory Medicine, P.O. Box 208035, New Haven, CT 06520-8035, Phone: (203) 737-2089, Fax: (203) 785-5415, mark.shlomchik@yale.edu.

AUTHOR CONTRIBUTIONS: A.K. performed experiments; A.K., J.C. and M.J.S. designed experiments, interpreted data and wrote the manuscript; J.C. contributed key reagents

To overcome these issues, we have used an IgM BCR B1–8 transgenic (Tg) mouse (6, 7). The Tg encodes a germline Vh186.2 rearrangement that is common in the anti-nitrophenyl (NP) response when combined with the 2–3% of Tg B cells expressing Vλ1. Such B cells in the Tg mice mount a vigorous GC response to NP-CGG immunization (6, 7). We first examined B cell signaling in freshly isolated splenic Ag-specific (i.e. $V\lambda1^+$) GC (peanut agglutinin, PNA^+) and "non-GC" (PNA^-) cells that were immediately fixed, followed by flow cytometric analysis of phosphorylated proteins (fig. S1A, B and see (8)). In immunized mice, non-GC cells are mainly non-responding bystander cells, and serve as an internal control, used in addition to naïve splenocytes. Naïve cells demonstrated basal tyrosine phosphorylation of the tyrosine kinase Syk (p-Syk, Y352) and its substrate, BLNK (p-BLNK, Y84) (fig. 1A), both proximal signal transducer elements of the BCR, results consistent with genetic and inhibitor studies (9, 10). GC B cells, however, had little detectable p-Syk or p-BLNK and much reduced total phosphotyrosine (p-Tyr), compared to either non-GC or naïve Ag-specific B cells (fig. 1A). In contrast, p-p38 (T180/Y182), p-ribosomal S6 (S235/236) and p-Akt (T308), were present in GC cells at similar or higher levels compared to control cells (fig. S1C).

Lack of BCR signaling could be explained by low in vivo Ag exposure or inherent resistance to BCR signals. To distinguish these possibilities, we stimulated splenocytes from d13 post-immunization (fig. S2A) with the monoclonal anti-IgM, b.7–6 (Fig. 1B), F(ab')2 anti-IgM or NP-BSA (fig. S2B,C). In contrast to non-GC cells, GC B cells demonstrated little if any induction of several phosphoproteins downstream of the BCR, suggesting that they were inherently antigen-refractory.

To evaluate BCR downregulation, we stimulated GC B cells directly with fluorescently labeled anti-IgM, which allowed us to electronically gate the analysis on cells with equivalent surface Ig levels (fig. S3A). Such GC cells again showed little induction of phosphoproteins compared to the non-GC cells with equivalent BCR expression. At 15 min post-stimulation GC B cells still did not contain elevated p-Syk, excluding kinetic differences (fig. S3B). >97% of the cells were still viable at the end of stimulatory cultures (fig. S4A), and consistent with this, GC cells were not inert--they generated p-Erk and p-p38 in response to PMA/ionomycin stimulation, which bypasses the BCR (fig. S2D). Furthermore, resistance to BCR-mediated generation of p-Syk was not a general property of activated B cells (fig. S4B).

In order to assess more proximal BCR signaling events, we evaluated basal phosphorylation of CD79, which is part of the BCR complex. GC cells had about half the amount of total CD79 compared to resting B cells (fig. S5A–C) as expected, because GC cells have less surface Ig (fig. S3A). Upon stimulation with anti-IgM, only non-GC and naïve B cells showed an increase in the amount of p-CD79, revealing a defect at the earliest measurable events of BCR signaling (fig. S5A–C).

Heightened phosphatase activity could explain the failure of GC B cells to accumulate increased tyrosine-phosphorylated CD79, Syk and BLNK (11, 12). We examined effects of Tyr phosphatase inhibition with H_2O_2. Exposure of GC B cells to H_2O_2 (fig. S6A) resulted in increased phosphorylation of Syk in non-GC cells, as reported (10). P-Erk, which is presumably downstream of Syk activation, was similarly affected, as were total p-Tyr levels. Notably, H_2O_2 rescued substantial p-Syk, p-Erk and p-Tyr expression in GC cells. Phosphorylation was somewhat higher in the non-GC cells, however, particularly at early time points. These data suggest that established phosphatase activity restrains spontaneous phosphorylation in GC B cells.

Consistent with higher Tyr-phosphatase activity, maximal phosphorylation in the GC required a higher concentration of H_2O_2 compared to non-GC B cells (Fig. 2A). To determine if H_2O_2 directly disinhibited BCR signaling, we pretreated splenocytes of immunized animals with a suboptimal concentration of H_2O_2 prior to anti-IgM stimulation. Such pretreatment synergistically enhanced BCR-induced Syk phosphorylation compared to anti-IgM or H_2O_2 alone (Fig. 2B). Treatment with anti-IgM and H_2O_2 (Fig. 2C,D) also synergistically elicited, more Ca^{2+} flux in both GC and non-GC cells compared to either anti-IgM or H_2O_2 alone; anti-IgM alone stimulated little Ca^{2+} flux in GC cells. The response to ionomycin showed that GC cells are at least as equipped to flux Ca^{2+} as non-GC cells (Fig. 2E). These results indicate that phosphatase activity limits the ability of GC B cells to carry out Tyr phosphorylation and Ca^{2+} flux in response to BCR stimulation.

To assess this, we measured both Tyr and Ser/Thr phosphatase activity in lysates from purified GC, non-GC and naïve B cells. As predicted, there was more Tyr and Ser/Thr phosphatase activity in the GC than naïve cells (fig. S6B). The finding of increased Ser/Thr phosphatase activity may be connected to impaired GC B cell generation of p-Erk and pp38 in response to BCR ligation (Fig. 1B). Although this could have been due to a block in proximal BCR signaling, there was also less Erk and p38 phosphorylation evident upon PMA/ionomycin stimulation in GC B cells (fig. S2D), consistent with increased Ser/Thr phosphatase activity.

We next examined whether SHP-1 (SH2 domain-containing phosphatase-1), a Tyr phosphatase known to regulate BCR signaling upon BCR ligation (13–15), may be responsible for reduced GC BCR signaling. Possible SHP-1 substrates include CD79, Syk, Vav, BLNK and CD22 (16). Furthermore, we investigated SHIP-1 (SH2 domain-containing inositol 5 phosphatase), which also regulates BCR signaling (17, 18) as well as Src family members because they can exert negative effects on BCR signaling (19). The activity of these proteins is increased by phosphorylation (20, 21). We found more p-SHIP-1 (Y1020) and p-SHP-1 and p-SRC (Y416) in unstimulated GC, compared to non-GC and naive (Fig. 3A,B and fig. S6C) B cells. Ex-vivo stimulation with anti-IgM increased phosphorylation of SHP-1, SHIP-1 and Src proteins (most likely Lyn) in non-GC and naïve B cells, reflecting normal regulation of signaling (15, 19, 20). P-SHIP-1, p-SHP-1 and p-Src did not rise in anti-IgM-stimulated GC B cells, however, and in fact consistently decreased upon BCR ligation.

SHP-1 (15) and SHIP-1 (22) are constitutively associated with the BCR in resting cells,. Unstimulated GC B cells demonstrated more SHP-1/BCR (Fig. 3C,D and fig. S7A,B) and SHIP-1/BCR (fig. S7C) co-localization than did non-GC cells. BCR ligation resulted in brisk dissociation of both SHP-1 and SHIP-1 from BCR in non-GC cells. In these cells BCR and SHP-1 relocalized to opposite poles of the cell, consistent with biochemical analysis of resting B cells (15). This dissociation was sustained for SHP-1 but transient for SHIP-1. In contrast, GC B cells barely showed any dissociation upon BCR ligation, though BCR/SHP-1 co-localization was reduced in a minor subset, albeit with slower onset and less sustained duration than in non-GC cells (Fig. 3D, fig. S7B, and see below). The differential localization of phosphatases in GC versus non-GC cells is further consistent with the regulation of BCR signaling in GC B cells by phosphatases.

To determine importance of SHP-1 in B cells during GC responses, we crossed SHP-$1^{fl/fl}$ (23) with a new Tg strain (hCD20. TamCre) that allows B cell-specific inducible Cre action (fig. S8A–C). B cell SHP-1 expression was reduced by injecting tamoxifen at d11-d13 after immunization (fig. S8A–C). This resulted in marked reduction of GC B cell frequencies (Fig. 3E,F), indicating that SHP-1 and presumably regulation of BCR signaling is required for maintaining the GC reaction.

If GC BCRs do not signal, then how does affinity-based selection occur? We did observe a small fraction of GC B cells in which Syk is phosphorylated. (fig. S5D) and SHP-1 relocalized (fig. 3D and fig. S7B) upon BCR ligation. We thus tested whether BCR signal transduction was cell cycle-dependent. BCR ligation induced p-Syk only in GC cells within the G2/M phase (Fig. 4A,B). Commensurate with this, we found that dissociation of BCR and SHP-1 occurred in G2; the amount of total SHP-1 was also substantially reduced in this phase, but returned to normal levels at M phase (Fig. 4C,D,E,F and fig S7D,E).

The discovery that most highly proliferative GC B cells undergoing Ag-driven selection cannot execute BCR signaling was contrary to expectations. This post-translational strategy for constraining signaling makes sense, however, as it could quickly be altered as cells progress through cycle or in response to other signals. These studies highlight a switch that gates early events in BCR signaling and which can be modified in GC B cells.

How, then, might affinity-based selection work? We suggest a model in which B cells integrate both T cell-derived and BCR signals in a cell-cycle dependent manner. Studies suggest that individual BCRs are dedicated to either BCR signaling or Ag presentation, with only the former depending on canonical p-CD79 generation (24). GC BCRs, which do not generate p-CD79, may thus favor Ag presentation. Since BCR Ag capture is affinity-dependent (25), more avid B cells would win out in a competition to gain T cell-dependent survival signals. This would explain positive selection in the absence of outright BCR signaling.

Nonetheless, BCR signaling may be important at key times during GC B cell proliferative cycling. B cells must test their affinity with each round of somatic hypermutation (26). Possibly, testing of mutant phenotypes occurs once per cell division, with the quality of BCR signaling determining the likelihood of completing mitosis and/or subsequent survival. Even in G2, the threshold for effective Ag sensing appears elevated, thus favoring selection of higher affinity B cells.

Supplementary Material

Refer to Web version on PubMed Central for supplementary material.

Acknowledgments

We thank A. Haberman for critical reading of the manuscript; J. Bezbradica for assistance and advice on western blotting, immunoprecipitation, and LiCor imaging; and G. Nolan for advice and protocols for flow cytometric detection of intracellular phosphoproteins. The data are tabulated in the main paper and in the Supporting Online Material. This work was supported by National Institutes of Health Grants AI43603 and AR44077 (to M.J.S.).

References and Notes

1. MacLennan IC. Germinal centers. Annu Rev Immunol. 1994; 12:117. [PubMed: 8011279]
2. Allen CD, Okada T, Cyster JG. Germinal-center organization and cellular dynamics. Immunity. Aug.2007 27:190. [PubMed: 17723214]
3. Martin SW, Goodnow CC. Burst-enhancing role of the IgG membrane tail as a molecular determinant of memory. Nat Immunol. Feb.2002 3:182. [PubMed: 11812996]
4. Waisman A, et al. IgG1 B cell receptor signaling is inhibited by CD22 and promotes the development of B cells whose survival is less dependent on Ig alpha/beta. J Exp Med. Apr 16.2007 204:747. [PubMed: 17420268]
5. Wakabayashi C, Adachi T, Wienands J, Tsubata T. A distinct signaling pathway used by the IgG-containing B cell antigen receptor. Science. Dec 20.2002 298:2392. [PubMed: 12493916]

6. Anderson SM, et al. Taking advantage: high-affinity B cells in the germinal center have lower death rates, but similar rates of division, compared to low-affinity cells. J Immunol. Dec 1.2009 183:7314. [PubMed: 19917681]
7. Anderson SM, Tomayko MM, Ahuja A, Haberman AM, Shlomchik MJ. New markers for murine memory B cells that define mutated and unmutated subsets. J Exp Med. Sep 3.2007 204:2103. [PubMed: 17698588]
8. See Supporting Online Materials (SOM) for Methods.
9. Cornall RJ, Cheng AM, Pawson T, Goodnow CC. Role of Syk in B-cell development and antigen-receptor signaling. Proc Natl Acad Sci U S A. Feb 15.2000 97:1713. [PubMed: 10677523]
10. Wienands J, Larbolette O, Reth M. Evidence for a preformed transducer complex organized by the B cell antigen receptor. Proc Natl Acad Sci U S A. Jul 23.1996 93:7865. [PubMed: 8755568]
11. Bolland S, Pearse RN, Kurosaki T, Ravetch JV. SHIP modulates immune receptor responses by regulating membrane association of Btk. Immunity. Apr.1998 8:509. [PubMed: 9586640]
12. Zhang J, Somani AK, Siminovitch KA. Roles of the SHP-1 tyrosine phosphatase in the negative regulation of cell signalling. Semin Immunol. Aug.2000 12:361. [PubMed: 10995583]
13. Cornall RJ, et al. Polygenic autoimmune traits: Lyn, CD22, and SHP-1 are limiting elements of a biochemical pathway regulating BCR signaling and selection. Immunity. Apr.1998 8:497. [PubMed: 9586639]
14. Cyster JG, Goodnow CC. Protein tyrosine phosphatase 1C negatively regulates antigen receptor signaling in B lymphocytes and determines thresholds for negative selection. Immunity. Jan.1995 2:13. [PubMed: 7600299]
15. Pani G, Kozlowski M, Cambier JC, Mills GB, Siminovitch KA. Identification of the tyrosine phosphatase PTP1C as a B cell antigen receptor-associated protein involved in the regulation of B cell signaling. J Exp Med. Jun 1.1995 181:2077. [PubMed: 7539038]
16. Tamir I, Dal Porto JM, Cambier JC. Cytoplasmic protein tyrosine phosphatases SHP-1 and SHP-2: regulators of B cell signal transduction. Curr Opin Immunol. Jun.2000 12:307. [PubMed: 10781410]
17. Liu Q, et al. The inositol polyphosphate 5-phosphatase ship is a crucial negative regulator of B cell antigen receptor signaling. J Exp Med. Oct 5.1998 188:1333. [PubMed: 9763612]
18. Okada H, et al. Role of the inositol phosphatase SHIP in B cell receptor-induced Ca2+ oscillatory response. J Immunol. Nov 15.1998 161:5129. [PubMed: 9820480]
19. Dal Porto JM, et al. B cell antigen receptor signaling 101. Mol Immunol. Jul.2004 41:599. [PubMed: 15219998]
20. Tamir I, et al. The RasGAP-binding protein p62dok is a mediator of inhibitory FcgammaRIIB signals in B cells. Immunity. Mar.2000 12:347. [PubMed: 10755621]
21. Zhang Z, Shen K, Lu W, Cole PA. The role of C-terminal tyrosine phosphorylation in the regulation of SHP-1 explored via expressed protein ligation. J Biol Chem. Feb 14.2003 278:4668. [PubMed: 12468540]
22. Phee H, Rodgers W, Coggeshall KM. Visualization of Negative Signaling in B Cells by Quantitative Confocal Microscopy. Mol Cell Biol. Dec 15.2001 21:8615. [PubMed: 11713294]
23. Pao LI, et al. B Cell-Specific Deletion of Protein-Tyrosine Phosphatase Shp1 Promotes B-1a Cell Development and Causes Systemic Autoimmunity. Immunity. 2007; 27:35. [PubMed: 17600736]
24. Hou P, et al. B cell antigen receptor signaling and internalization are mutually exclusive events. PLoS Biol. Jul.2006 4:e200. [PubMed: 16719564]
25. Batista FD, Neuberger MS. B cells extract and present immobilized antigen: implications for affinity discrimination. Embo J. 2000; 19:513. [PubMed: 10675320]
26. Shlomchik MJ, Watts P, Weigert MG, Litwin S. “Clone”: A Monte-Carlo Computer Simulation of B Cell Clonal Expansion, Somatic Mutation and Antigen-Driven Selection. Curr Top Micro Immunol. 1998; 229:173.
27. Chen J, et al. Immunoglobulin gene rearrangement in B cell deficient mice generated by targeted deletion of the JH locus. Int Immunol. Jun.1993 5:647. [PubMed: 8347558]
28. Lang P, et al. TCR-induced transmembrane signaling by peptide/MHC class II via associated Ig-alpha/beta dimers. Science. Feb 23.2001 291:1537. [PubMed: 11222857]

29. Nakamura T, et al. Suppression of humoral immunity by monoclonal antibody to CD79b, an invariant component of antigen receptors on B lymphocytes. Int J Hematol. Jul.1996 64:39. [PubMed: 8757966]

30. Shlomchik MJ, Zharhary D, Saunders T, Camper SA, Weigert MG. A rheumatoid factor transgenic mouse model of autoantibody regulation. Int Immunol. Oct.1993 5:1329. [PubMed: 8268138]

31. Ahuja A, et al. Depletion of B cells in murine lupus: efficacy and resistance. J Immunol. Sep 1.2007 179:3351. [PubMed: 17709552]

32. Kaplan DH, Jenison MC, Saeland S, Shlomchik WD, Shlomchik MJ. Epidermal langerhans cell-deficient mice develop enhanced contact hypersensitivity. Immunity. Dec.2005 23:611. [PubMed: 16356859]

33. Wen F, et al. Expression of conditional cre recombinase in epithelial tissues of transgenic mice. Genesis. Feb.2003 35:100. [PubMed: 12533792]

34. Srinivas S, et al. Cre reporter strains produced by targeted insertion of EYFP and ECFP into the ROSA26 locus. BMC Developmental Biology. 2001; 1:4. [PubMed: 11299042]

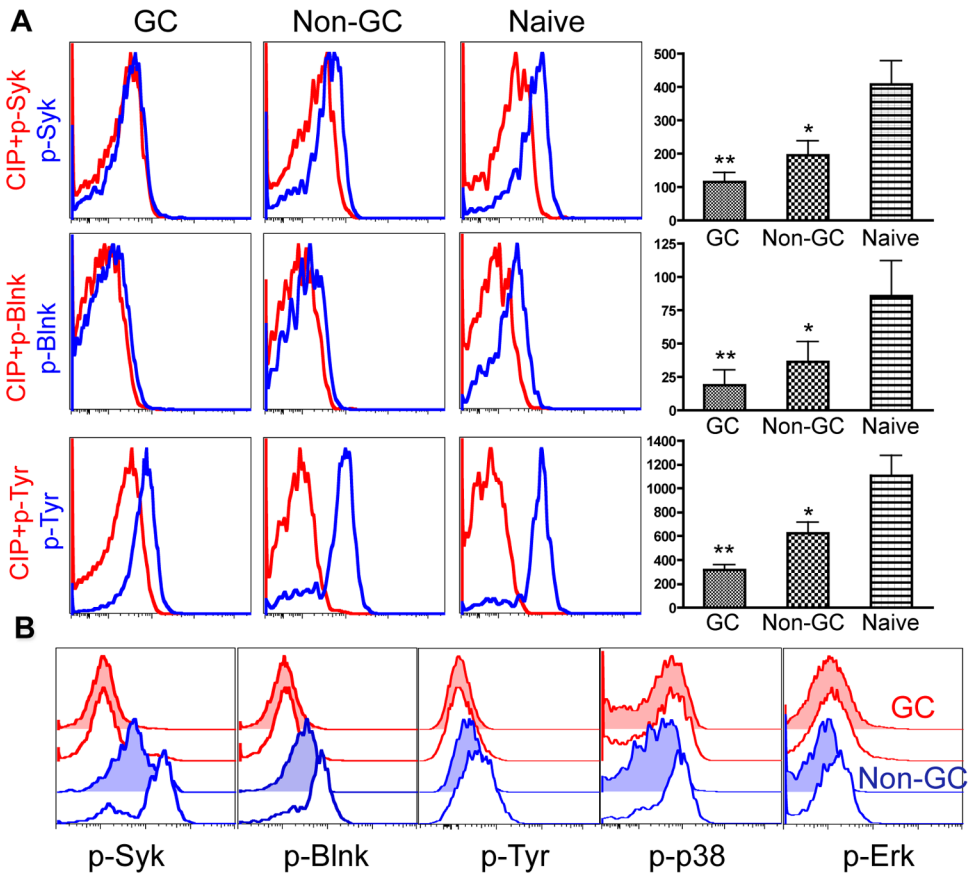

Fig. 1.

Spontaneous and ligand-induced BCR signaling in GC, non-GC and resting B cells. **(A)** BCR-linked basal signaling in gated populations of GC, non-GC and naïve B cells from instantly-fixed total splenocytes harvested from d13 NP-CGG immunized mice (fig. S1). Fixed cells were treated with or without calf intestinal phosphatase (CIP), then labeled with antibodies specific for phosphorylated proteins. (**A)** Histograms show representative results of tyrosine phosphorylation from CIP-treated (red line) and untreated (blue line) cells, overlaid for direct comparison. y-axes show relative cell number. Bar charts are net median fluorescence intensity (MFI) indicating basal phosphorylation calculated by subtracting MFI of CIP treated from CIP untreated cells. Error bars are SEM from at least 5 independent experiments each using cells pooled from spleens of at least two mice for each group. * $p < 0.05$ and ** $p < 0.01$ MFI of GC or non-GC compared to naïve. **(B)** Response of GC, non-GC and resting B cells to BCR ligation. Total splenocytes from d13 NP-CGG immunized mice were stimulated ex-vivo with anti-μ (15μg/ml) for 5 minutes. Levels of Syk, Blnk, Tyr, p38 and Erk phosphorylation in gated GC and non-GC were measured. Profiles of GC unstimulated (red filled area), GC anti-IgM stimulated (red open line), non-GC unstimulated (blue filled area) and non-GC anti-IgM stimulated (blue open line) are overlaid for direct comparison.

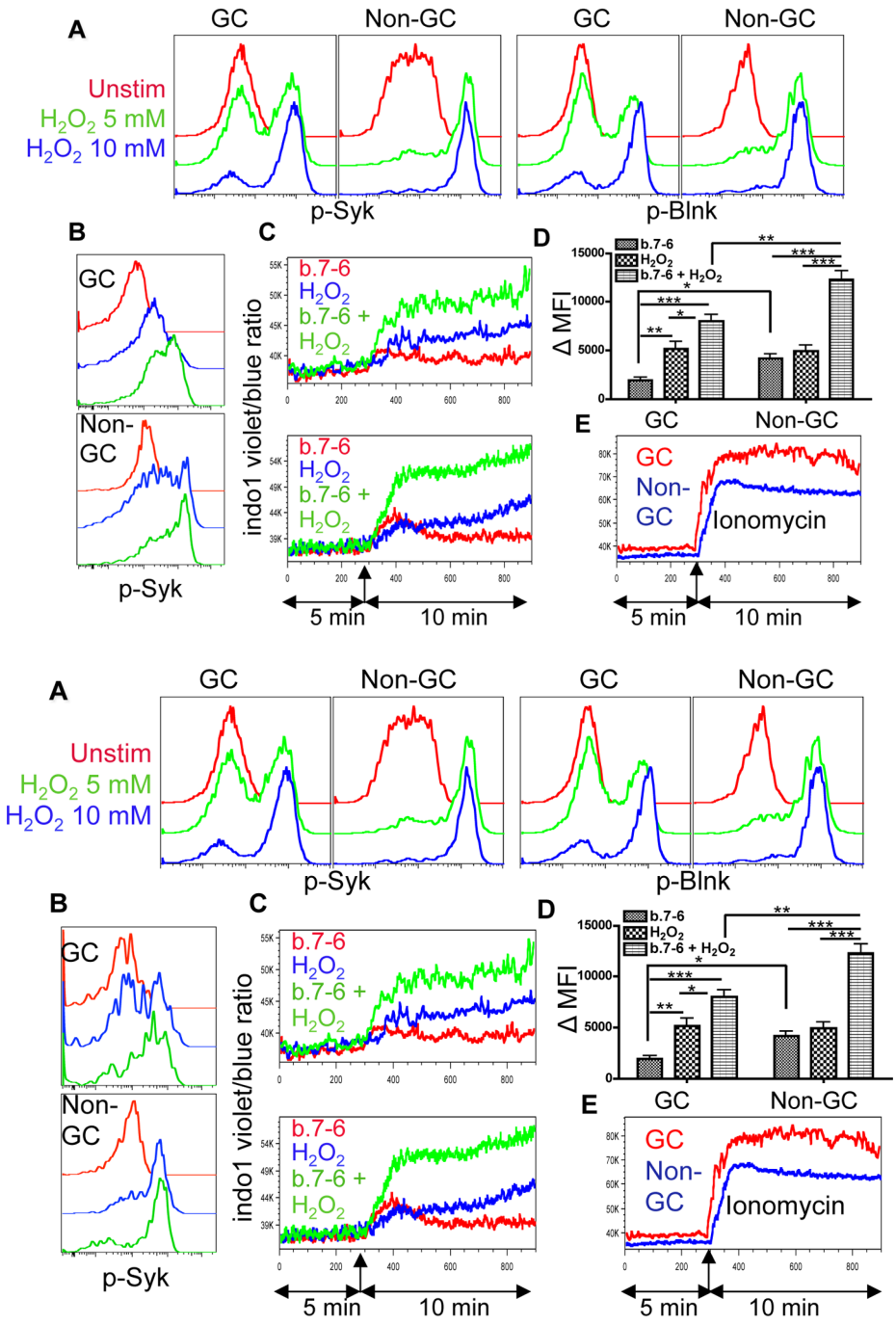

Fig. 2.

Analysis of phosphatase-dependent regulation of BCR signaling in GC cells. **(A)** Total splenocytes from d13 NP-CGG immunized mice were stimulated with 5mM (green line) or 10mM (blue line) H_2O_2 followed by detection of p-Syk and p-Blnk by flow cytometry in gated GC and non-GC Ag-specific cells. Figure is representative of 3 independent trials each of 3 mice. (**B)** Assessment of interaction between BCR ligation and phosphatase inhibition. Total splenocytes from immunized mice as in **(A)** were stimulated with 15μg/ml anti-IgM (red), 5mM H_2O_2 (blue) or both (green), and generation of p-Syk was assessed by flow cytometry. Representative of 3 or more experiments. (**C**) Indo1AM-loaded total splenocytes

from immunized mice were stimulated with 15μg/ml anti-IgM (red), 5 mM H_2O_2 (blue) or both (green). Stimuli were added after acquiring events for 5 minutes to establish a basal level. Profiles of stimulants in gated GC (top) and non-GC (bottom) populations are overlaid. y-axis is indo1 violet to blue fluorescence ratio, an indicator of intracellular Ca^{2+} levels. (**D)** Compiled responses of GC and non-GC cells treated as in (**C).** Background-subtracted MFI was calculated from gates drawn before (180s time, background) and after (200s time, beginning at approximately the initial peak of response to anti–μ) stimulation. Bars show mean + SEM of net MFI from 4 independent experiments. *$p < 0.05$, **$p < 0.01$, ***$p < 0.001$. (**E**) Ca^{2+} flux to ionomycin, used as positive control indicating equal responsiveness of GC and non-GC cells.

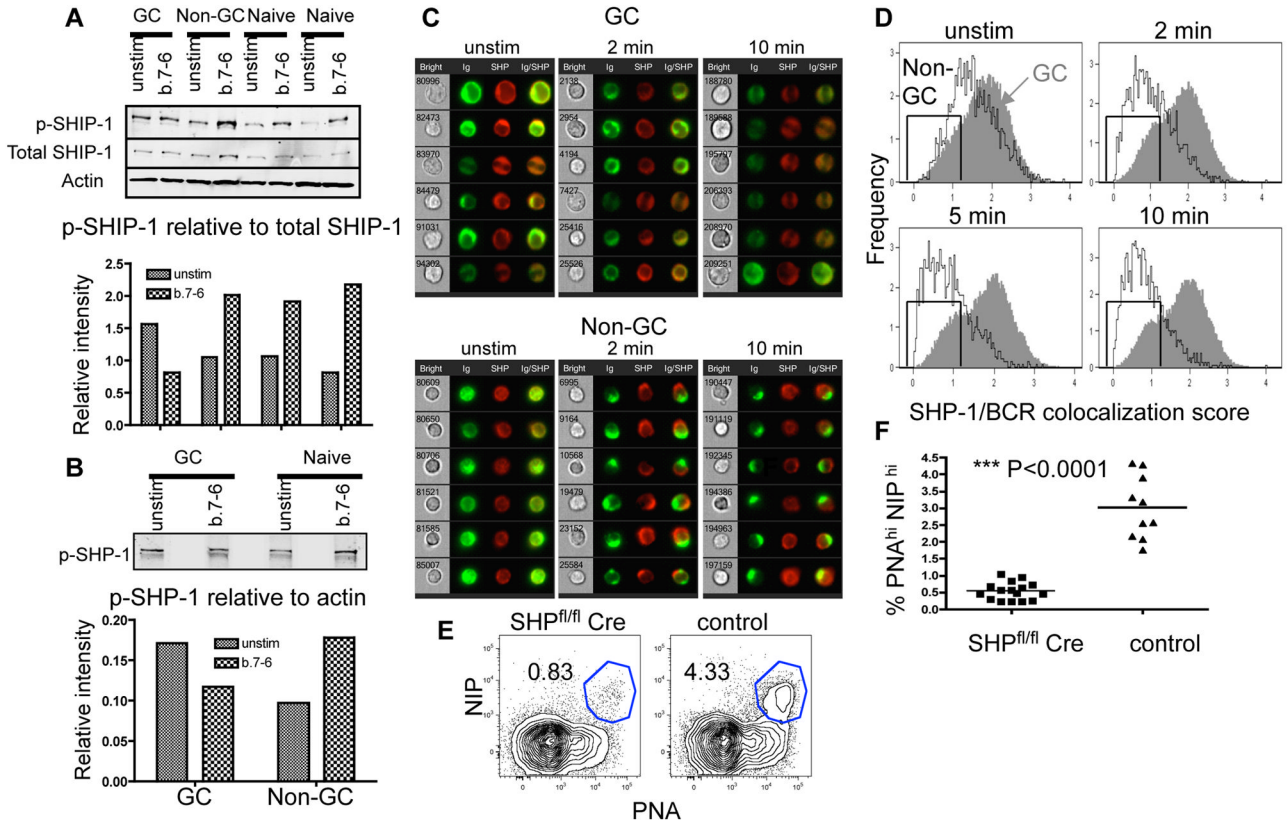

Fig. 3.

Differences in phosphorylation and localization of SHIP-1 and SHP-1 in GC and naïve B cells after and without BCR ligation. (**A)** Top: SHIP-1 phosphorylation (Y1020) was determined by Western blot of lysates from unstimulated and anti-IgM stimulated (5 min) FACS-sorted GC, non-GC and naïve B cells. β-actin was used as a loading control. Bottom: Quantitation of blot shown in top is median fluorescence intensity (MFI) of gated p-SHIP-1 bands relative to total SHIP-1. Blots shown are representative of 3 similar experiments. **(B)** Top: Tyrosine phosphorylation of SHP-1 was determined by immunoprecipitation of total SHP-1 in FACS-sorted GC and naïve B cells both unstimulated and after 2 minutes of anti-IgM stimulation, followed by blotting with anti-pTyr (4G10). Bottom: Quantitation of blots shown in top is MFI of gated p-SHP-1 relative to β-actin, which was determined by western blot on parallel samples of the same lysates. Data representative of 4 similar experiments: **(C, D)** High throughput imaging cytometric analysis of SHP-1/BCR association. Total splenocytes were either left unstimulated or stimulated with anti-IgM (b.7–6) for 2, 5, 10, 15 and 30 minutes; see fig. S7A for 15 and 30 min summary data. **(C)** Representative images of GC (top row) and Non-GC (bottom row) B cells captured by the Amnis Imagestream X. (**D**) Co-localization of SHP-1 and BCR was measured in gated non-GC ($\lambda_1^+PNA^{lo}$) and GC ($\lambda_1^+PNA^{hi}$) as similarity scores in GC (shaded) and non-GC (open) B cells at multiple time points with respect to BCR ligation (all time points summarized in fig. S7A). The box depicts a gate drawn at <1.2 similarity, which was used to calculate the % of GC and non-GC cells demonstrating substantial SHP-1/BCR dissociation at various times after BCR ligation (fig. S7B). (**E, F**) Effect of deletion of SHP-1 in B cells on the ongoing GC response. The strategy for tamoxifen-induced deletion using a new B cell-specific inducible Cre (hCD20-TamCre) and SHP-$1^{fl/fl}$ mice is detailed in fig. S8. SHP-$1^{fl/fl}$ mice with or without (control) the Cre Tg were immunized with NP-CGG, treated from d 9–12 with tamoxifen and then analyzed at d 14. (**E**) Representative flow cytometric analysis of

splenocytes from experimental (left) and control (right) mice, detecting Ag-specific GC cells as PNA^{+}/NIP^{+} among gated $B220^{+}$ B cells. Numbers are percentages of B cells in the gate. (**F**) Data from 3 independent experiments showing loss of GC B cells (B220+PNA+NIP+) upon SHP-1 deletion in B cells.

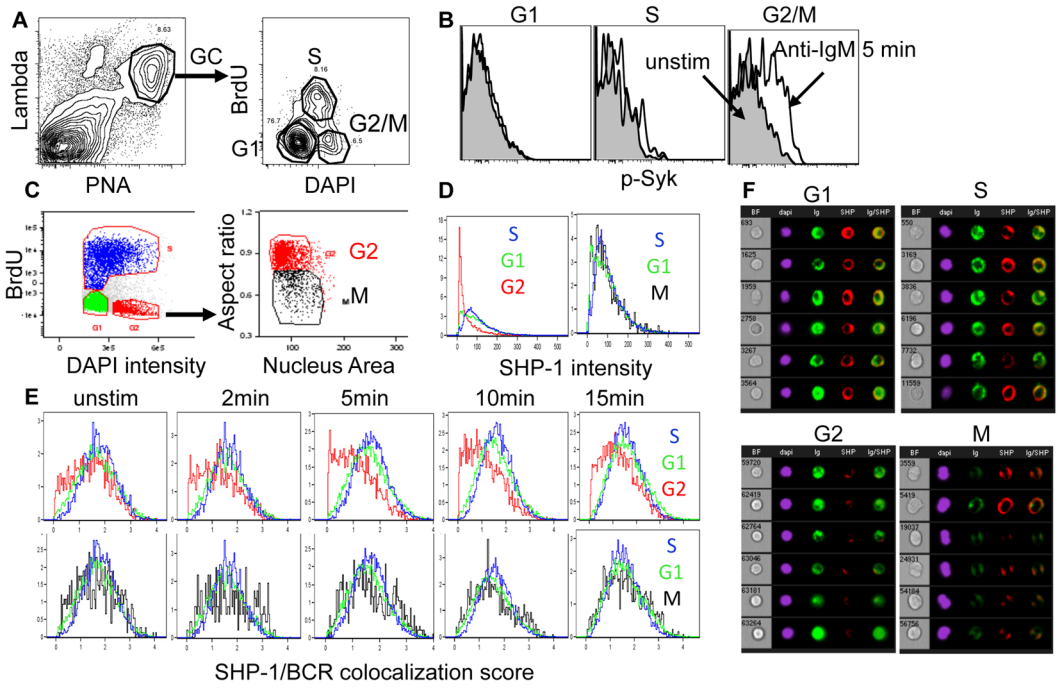

Fig. 4. BCR signal transduction in GC B cells at the G2/M phase of cell cycle

Mice at d13 post-immunization with NP-CGG were injected i.v. once with 3 mg of 5-Bromo-2′-deoxyuridine (BrdU) and sacrificed 1 h later. Splenocytes were isolated, and either treated with anti-IgM or not for 5′ and then fixed and stained as described in Materials and Methods. (**A**) Flow cytometry gating to identify GC B cells (left panel) and then separate them into cell cycle compartments based on DAPI and BrdU staining (right panel). (**B**) Phosphorylation of Syk in response to BCR ligation was measured in gated populations based on (**A**) and as labeled: G1 (left), S (center) and G2/M (right). Histograms of p-Syk staining in unstimulated cultures are grey-filled and of stimulated cultures are open. Data are representative of four independent mice from two independent experiments, all with similar results. (**C–F**) GC cells were analyzed on the Imagestream X for SHP-1 intensity and SHP-1/BCR colocalization during different phases of the cell cycle. GC B cells were prepared and treated as in (**A**) but analyzed on the Imagestream after staining as in Fig. 3. (**C**) DAPI and BrdU identify G1, S and G2/M phases. G2 and M phases were separated based on nuclear area and aspect ratio. (**D**) Analysis of total SHP-1 expression as a function of cell cycle. (**E, F**) Analysis of SHP-1/BCR colocolazation as a function of cell cycle. during the G2 phase compared to G1 and S phases. However, SHP-1 level increased back at the M phase. Moreover, ex vivo stimulation resulted in time-dependent dissociation of SHP-1 from the BCR only during the G2 phase. Data are representative of 2 experiments.